Journal of Research and Applications in Mechanical Engineering
ISSN: 2229-2152 (Print); 2697-424x (Online)
(2024) Vol. 12, No. 2, Paper No. JRAME-24-12-024
[DOI: 10.14456/jrame.2024.24]

Research Article

Effect of Plane Walls on Flow Characteristics of Primary Jets Controlled by Secondary Flow

H. Tezuka[1]
K. Yabu[2]
K. Nishibe[3]
D. Kang[4]
K. Sato[2,*]
[1] *Mechanical Engineering Program in the Graduate School of Engineering, Kogakuin University, Tokyo 192-0046, Japan*
[2] *Department of Mechanical System Engineering, Kogakuin University, Tokyo 192-0046, Japan*
[3] *Department of Mechanical Engineering, Tokyo City University, Tokyo 158-8557, Japan*
[4] *Department of Mechanical Engineering, Saitama University, Saitama 338-8570, Japan*

Received 27 September 2023
Revised 27 December 2023
Accepted 1 January 2024

Abstract:
The method for controlling the direction of primary jets by secondary flow is called fluid thrust vectoring. It was originally studied for application in aircraft attitude control, where it was expected to reduce fuel consumption and improve motion performance. It has been demonstrated that the direction of the primary jet can be adjusted by adjusting the momentum of the secondary flow generated near a curved surface (Coanda surface), such as a cylinder. However, there is limited research applying the abovementioned method to fields such as aviation for flows other than external flows. To use this method for internal flows, such as airflow control in a room, knowledge of the geometric boundaries near the jet flow is required. That is, the interference problem between the jet and wall boundaries must be investigated to realize jet direction control using secondary flows in various fields. Thus, this study investigated the effects of wall length and step height (offset ratio) on the flow characteristics of jets controlled by secondary flow near the Coanda surface. Typical flow patterns are presented in this paper, and the jet deflection characteristics are discussed primarily through flow visualization and velocity distribution measurements.

Keywords: *Jet vectoring, Coanda effect, Secondary flow, Wall boundaries, Offset ratio*

1. Introduction

Fluidic thrust vectoring [1-17], which is achieved by adjusting the momentum of a secondary flow generated near a cylindrical surface, is a control technique that utilizes the Coanda effect, in which the jet adheres to a curved surface. It has attracted attention because of its advantages over conventional mechanical thrust vectoring, such as reduced equipment weight and a large deflection angle.

Mason and Crowther [1] attempted to control the direction of the primary jet using a continuous jet in a secondary flow near a Coanda surface and investigated the effect of the momentum ratio on the deflection characteristics through experiments and CFD. Their findings categorized the deflection characteristics of the jet into three: dead zone, control region, and saturation region. Recently, Watanabe et al. [2] and Tamanoi et al. [3] investigated the relationship between jet deflection angle and momentum ratio for various jet width ratios under the conditions of a constant Coanda surface radius and jet/suction secondary flow. The suction secondary flow was shown to be more suitable for jet deflection angle control than jet flow, and the effect of geometry on the jet deflection characteristics was also discussed.

* Corresponding author: K. Sato
E-mail address: at12164@ns.kogakuin.ac.jp

In addition, when a sidewall exists near the jet, the jet is attracted to the wall side, forming a recirculation zone and becoming a wall-attached jet, which is widely known as the Coanda effect [4-7]. In the future, fluidic thrust vectoring is expected to have applications outside the aeronautical field; in such situations, there will likely be many cases in which boundaries exist in the vicinity of the jet. For example, when applying fluidic thrust vectoring to internal flows, such as airflow control in homes and factories and in fluid machinery, the effect of sidewalls on the flow characteristics of the jet must be considered. Last year, experiments were conducted to clarify the flow characteristics of a jet near a plane wall by applying a steady jet, steady suction, and synthetic jet to a secondary flow with a cylindrical Coanda surface. It was found that the deflection angle of the jet near the plane wall can be controlled by the suction and synthetic jets, which are a steady secondary flow and secondary flow, respectively. Moreover, the jet can be deflected to the opposite side of the plane wall under certain conditions [6, 7]. However, the effectiveness of fluidic thrust vectoring near the sidewalls remains unclear.

This study is fundamental for the application of fluidic thrust vectoring near flat sidewalls. Furthermore, it attempts to elucidate the effect of finite-length flat sidewalls on the flow characteristics of a primary jet controlled by a secondary flow with a Coanda surface. The relationship between the jet deflection characteristics, relative length of the flat sidewalls, and offset ratio (the distance from the slot to the flat sidewall, which is nondimensionalized based on the slot width) was experimentally investigated under constant momentum ratios of the primary and secondary jets. Flow visualization observations were performed.

2. Experimental Methods

Fig. 1 shows a schematic of the experimental apparatus with air as the working fluid. It illustrates the equipment configuration used when applying a steady jet as the primary jet and steady suction as the secondary flow. For the primary jet, the flow was generated by a blower (U75-2-R313, Showa Denko) and emanated from the slot through a plenum tank and nozzle. A Coanda surface and a slot for the secondary flow were provided on the opposite direction to the plane wall of the slot outlet, and a steady secondary flow was generated by suction with a vortex blower (U2V-70S, Showa Denko). Because hysteresis generally occurs in jet phenomena, the experimental procedure in this study was unified as follows. First, a primary jet was generated by a blower. After confirming that the flow field was sufficiently developed, a secondary flow was suctioned by a blower. The momentum of each flow was regulated using an inverter and a valve. The flow field in the test section was sandwiched between two acrylic plates with dimensions of 1.0 m × 1.0 m in the x-y plane and 7.0×10^{-2} m in the z-axis. The length C and offset distance S of the flat sidewalls in the test section were variable parameters.

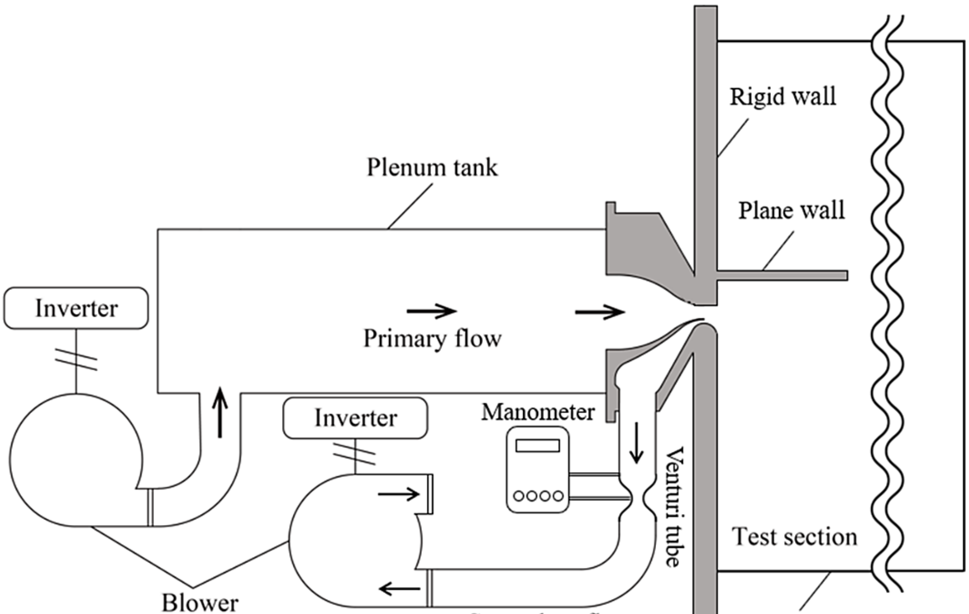

Fig. 1. Schematic of the experimental apparatus

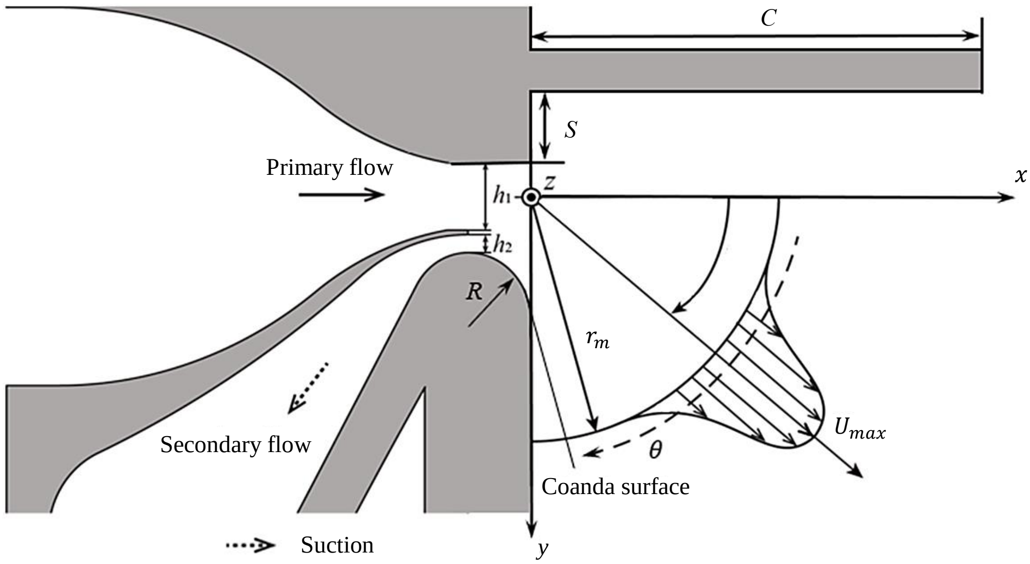

Fig. 2. Geometric shape of the slot

Fig. 2 shows a magnified view of the slot section. The slot widths of the primary and secondary jets are $h_1 = 1.0 \times 10^{-2}$ m and $h_2 = 2.0 \times 10^{-3}$ m, respectively, and the slot width ratio is constant at $h_2 / h_1 = 0.2$. The direction of the jet flow was controlled by interfering with the primary and secondary flows near a cylindrical Coanda surface with radius $R = 1.5 \times 10^{-2}$ m. In this study, the flow velocity measured at the center of the slot width and span was defined as the primary flow velocity U_1. $U_1 = 10.0$ m/s was constant, and in the presence of a secondary flow, $U_2 = 3.16$ m/s was tested with a momentum ratio $M_2 / M_1 = 0.02$. The primary jet flow velocity was set at the center of the slot outlet using an I-type probe (Kanomax 0251R-T5) on a hot-wire anemometer (Kanomax Smart-CTA 7250). The velocity setting of the secondary flow was subject to fluctuations owing to the mutual interference caused by the simultaneous suction of the primary jet and secondary flow. Therefore, a Venturi tube was installed between the secondary slot and the blower. Moreover, the differential pressure was measured with a manometer to determine the flow velocity at the slot outlet by measuring the flow rate in real time while the primary jet was blowing. The differential pressure manometer had a measurement range of 0 to 200.0 Pa and an accuracy of ± 0.25FS % ±1 dig. The I probe was placed parallel to the y- and z-axes when measuring the x-directional component of the jet and the overall velocity $|\boldsymbol{v}| = \sqrt{u^2 + v^2}$, respectively.

The Reynolds number Re, which was based on the primary jet velocity U_1 and slot width h_1, was $Re = 6.7 \times 10^3$. The maximum time resolution of the hot-wire anemometer was 20 kHz however was measured at 10 kHz. Although the flow focused on in this experiment was turbulent, the temporal resolution of the measurement device was sufficient because only time-averaged values were used. In the visualization observation experiment, the smoke generated by the smoke generator was fed from the blower inlet to the primary flow. The phenomena were captured using a 480-fps digital camera (SONY VLOGCAM ZV-1) with an exposure time of 1 / 50 s, employing a PIV laser as the light source.

3. Results and Discussion

Figs. 3-6 show the flow visualization observations obtained under the conditions of $R = 1.5 \times 10^{-2}$ m, $h_1 = 1.0 \times 10^{-2}$ m, $h_2 = 2.0 \times 10^{-3}$ m, and $U_1 = 10.0$ m/s. Fig. 3 shows the flow patterns without flat sidewalls, with (a) showing the case of a single primary jet (no secondary flow) and (b) depicting an example of jet direction control by a secondary suction flow ($M_2 / M_1 = 0.02$). In (a), the flow field is generally symmetrical about the x-axis; therefore, the jet moves straight ahead. By contrast, in (b), the primary jet flows along the Coanda surface due to the negative pressure created by the secondary suction flow. The jet is deflected, which is consistent with the results of previous studies [2-7, 13-16].

Fig. 4 shows an example of a typical flow pattern in the presence of a flat sidewall (c = 4.0 × 10^{-2} m, s = 2.0 × 10^{-2} m) near the slot. As shown in the previous figure, (a) and (b) show a single primary jet and an example of jet direction control (M_2 / M_1 = 0.02) by a secondary suction flow, respectively. In (a), the primary jet is deflected toward the flat sidewall of the plate due to the Coanda effect, whereas in (b), the secondary suction flow deflects the primary jet toward the opposite direction to the plane wall, even when a plane wall is present.

Fig. 5 (a) and (b) show the flow visualization observations highlighting the effect of the plane wall length on the flow pattern under the same offset ratio (S = 2.0 × 10^{-2}) as that in Fig. 4. Fig. 5 (a) shows an example with short sidewalls (C = 2.0) and (b) shows an example with long sidewalls (C = 20.0). In (a), the phenomena were photographed with an exposure time of 1/50 s, because the flow is essentially steady; while in (b), the flow pattern was photographed with an exposure time of 1 s, because unsteady phenomena are observed. Fig. 5 shows the velocity distribution (u/U_1) in the x-direction measured by the hot-wire anemometer. To clarify the jet deflection characteristics, the jet centers (the location of the maximum jet velocity) are as indicated by the red circles, and the time-averaged trajectory of the jet center are shown. However, since the flow direction cannot be determined by the hot-wire anemometer, the position of the maximum jet velocity near the slot cannot be regarded as the jet center in case (b). This reflects the complex behavior, and therefore, based on comprehensive judgment based on the photographs and movie obtained from the preliminary experiment, the position of the second peak occurrence in the x-directional velocity distribution are plotted as the position of the second peak in the x-directional velocity distribution, as indicated by the yellow circles. Here, it is assumed that this position is the time-averaged jet center. Under condition (a), the primary jet immediately flows along the cylinder surface due to the Coanda effect after slot exit, and is deflected to a higher degree to the opposite side of the plane wall without significant influence from the flat plate wall. By contrast, under the condition (b), the jet flows along the cylinder surface immediately after the slot due to the Coanda effect; however, it is pulled back downstream to the plane wall side. In condition (b), the jet is pulled back toward the plane wall immediately after the slot due to the Coanda effect, resulting in the smaller degree of jet deflection.

Fig. 6 shows examples of the observed behaviors for different offset ratios. The length of the flat sidewall is C = 1.2 × 10^{-1} m. In (a), the offset ratio of the flat sidewall is relatively small (S = 2.0 × 10^{-2} m), whereas in (b), the offset distance of the flat sidewall is relatively large (S = 6.0 × 10^{-1} m). Similar to Fig. 5, both jets are deflected toward the opposite side of plane wall immediately after slot exit. However, in (a), the entrainment flow is limited owing to the presence of the flat sidewall. Conversely, in case (b), the flat sidewall is far from the slot, and significant deflection toward the opposite side of plane wall is observed. This indicates that sufficient entrainment flow is supplied to the jet flow due to the reduced flat sidewall effect.

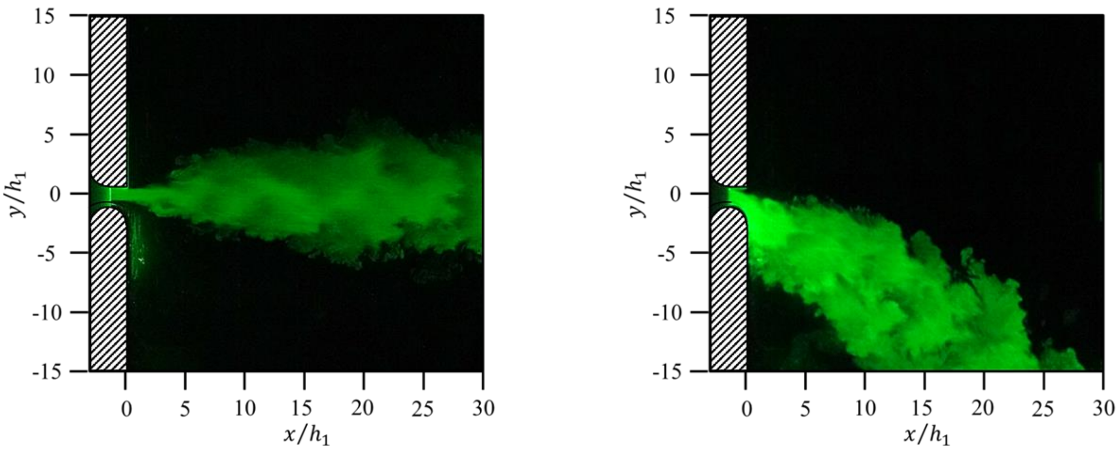

(a) Conditions with primary jet only

(b) Conditions with secondary suction flow applied (U_2 = 3.16 m/s, M_2 / M_1 = 0.02)

Fig. 3. Examples of the visualization observation of a typical flow pattern in the absence of flat sidewalls (h_1 = 1.0 × 10^{-2} m, h_2 = 2.0 × 10^{-3} m, U_1 = 10.0 m/s)

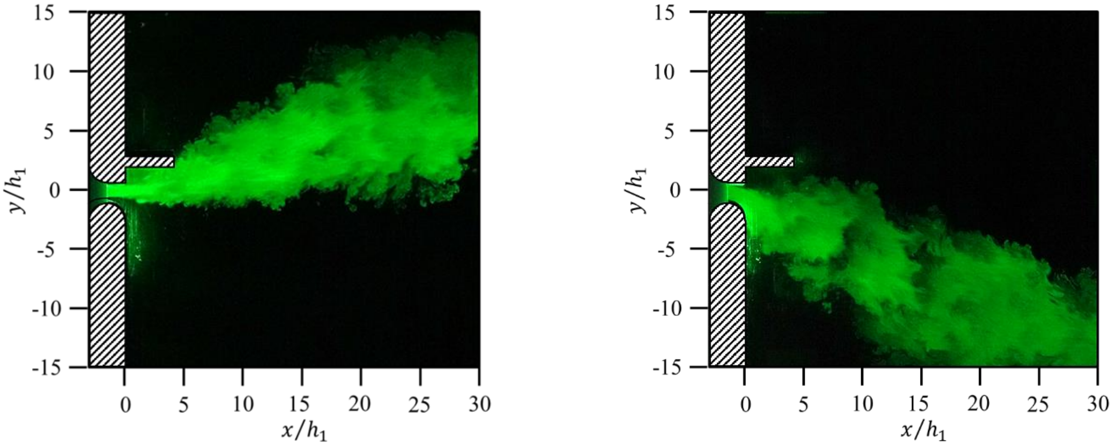

(a) Conditions with primary jet only

(b) Conditions with secondary suction flow applied (U_2 ＝3.16 m/s, M_2 / M_1 ＝ 0.02)

Fig. 4. Examples of the visualization observation of a typical flow pattern in the presence of flat sidewalls (h_1 = 1.0 × 10^{-2} m, h_2 = 2.0 × 10^{-3} m, U_1 = 10.0 m/s, c = 4.0 × 10^{-2} m, C = 4.0, s = 2.0 × 10^{-2} m, S = 2.0)

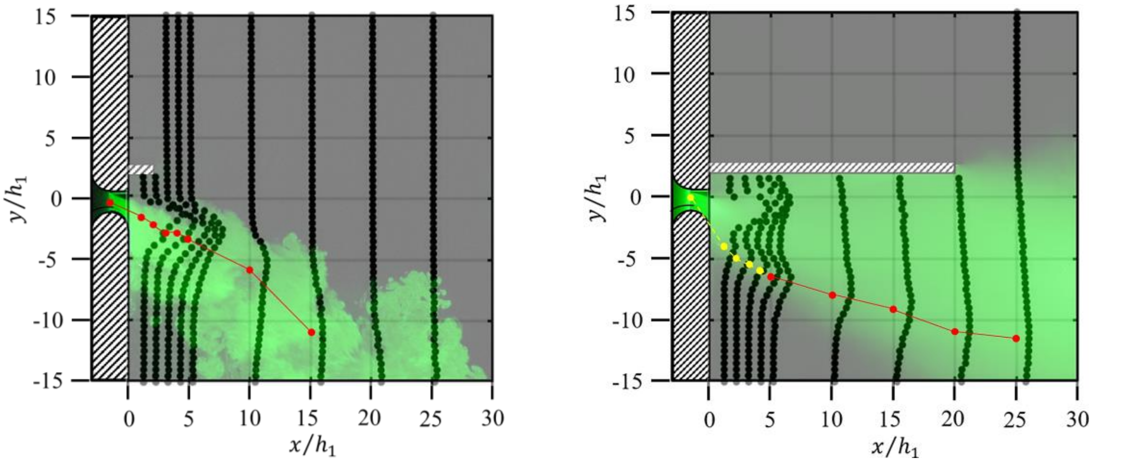

(a) Conditions with small flat sidewall length (c = 2.0 × 10^{-2} m, C = 2.0)

(b) Conditions with large flat sidewall length (c = 2.0 × 10^{-1} m, C = 20.0, Exposure time 1 s)

Fig. 5. Examples of the visualization observation showing the effect of relative flat sidewall length on jet deflection characteristics (h_1 = 1.0 × 10^{-2} m, h_2 = 2.0 × 10^{-3} m, U_1 = 10.0 m/s, U_2 ＝3.16 m/s, M_2 / M_1 ＝ 0.02, s = 2.0 × 10^{-2} m, S = 2.0)

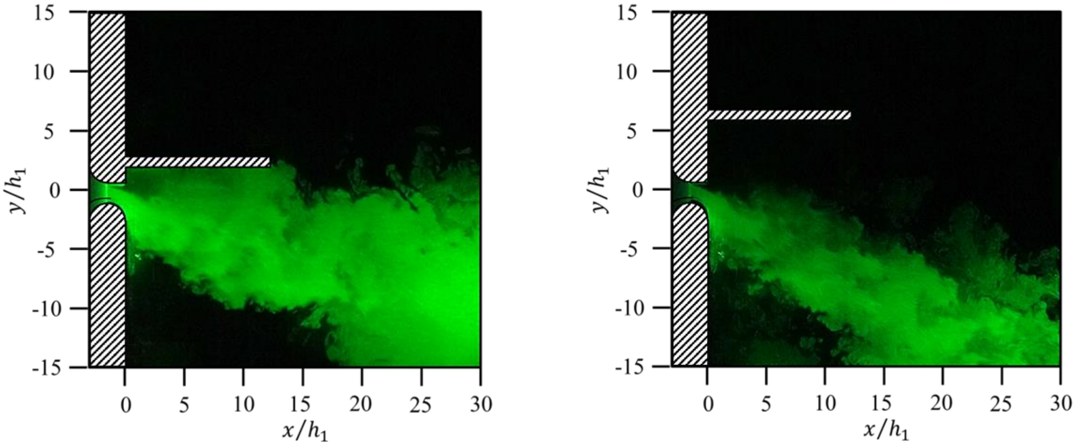

(a) Conditions with small offset distance
($s = 2.0 \times 10^{-2}$ m, $S = 2.0$)

(b) Conditions with large offset distance
($s = 6.0 \times 10^{-2}$ m, $S = 6.0$)

Fig. 6. Examples of the visualization observation showing the effect of offset ratio on jet deflection characteristics
($h_1 = 1.0 \times 10^{-2}$ m, $h_2 = 2.0 \times 10^{-3}$ m, $U_1 = 10.0$ m/s,
$U_2 = 3.16$ m/s, $M_2 / M_1 = 0.02$, $c = 1.2 \times 10^{-1}$ m, $C = 12.0$)

4. Conclusion

In this study, the effects of the relative length of the flat sidewalls and offset ratio on the deflection characteristics of the jet flow were clarified under the condition that the momentum ratio of the primary jet to that of the secondary flow is constant. Under conditions where a flat sidewall exists near the slot, the jet is attracted toward the sidewall when no secondary flow is used. By contrast, the secondary suction flow deflects the jet toward the opposite side of the plane wall, and the flow characteristics of the primary jet depend on the momentum of the secondary flow, relative length of the plane wall, and offset ratio. Furthermore, it was found that when the relative length of the flat sidewall is large, the jet is deflected toward the opposite side of the plane wall along the Coanda surface immediately. Then, the jet flow is pulled toward the flat sidewall again.

Acknowledgments

We would like to thank Mr. Yuki Watanabe and Mr. Yu Tamanoi (Kogakuin University graduate students) for their assistance in fabricating the experimental apparatus. This study was supported by JSPS KAKENHI Grant Number 23K17731 and a Hatakeyama Research Grant from the Turbomachinery Society of Japan.

Nomenclature

c	:	Length of the plane side wall [m]
C	:	Nondimensional length of the plane side wall ($=c/h_1$)
h_1	:	Primary slot width ($= 1.0\times10^{-2}$) [m]
h_2	:	Secondary slot width ($= 2.0\times10^{-3}$) [m]
i	:	1 for primary jet or 2 for secondary flow
M_i	:	Momentum of the primary or secondary flow at the slot exit ($= \rho U_i^{\,2} h_i$) [N]
R	:	Radius of the Coanda surface ($= 1.5\times10^{-2}$) [m]
Re	:	Reynolds number ($= U_1 h_1/\nu = 6.7\times10^3$) [-]
r_m	:	Radius of the velocity measurement arc ($= 1.5\times10^{-1}$) [m]
s	:	Distance from the primary slot to the plane side wall [m]
S	:	Offset ratio ($=s/h_1$)
u	:	Velocity in the x-direction [m/s]
U_i	:	Velocity of the primary or secondary flow at the slot exit [m/s]

U_{max} : Maximum velocity of the velocity distribution [m/s]
v : Velocity in the y-direction [m/s]
$|\boldsymbol{v}|$: Absolute value of the velocity at an arbitrary point [m/s]
x, y, z : Coordinate axis
z_h : Height of the test section (=7.0×10^{-2}) [m]
θ : Clockwise angle from the x-axis [deg]
ν : Kinematic viscosity (=1.5×10^{-5}) [m^2/s]
ρ : Fluid density [kg/m^3] (=1.5×10^{-5}) [m^2/s]

Subscripts
1 : Primary jet
2 : Secondary flow

References

[1] Mason MS, Crowther WJ. Fluidic thrust vectoring of low observable aircraft. CEAS Aerospace Aerodynamic Research Conference; 2002 Jun 10-12; Cambridge, United Kingdom. London: RaeS; 2002. p. 1-17.
[2] Watanabe Y, Sato K, Sato M, Nishibe K, Kang D, Yokota K. Vector control of jet flow using secondary excited jets. The 29th International Symposium on Transport Phenomena; 2018 Oct 30-Nov 2; Hawaii, USA.
[3] Tamanoi Y, Watanabe Y, Kobayashi R, Sato K. Control of jet flow direction. Proceedings of the 57th Annual Meeting of the Hokkaido Branch of the Japan Society of Mechanical Engineers; 2020 Mar 7; Hokkaido, Japan.
[4] Tezuka H, Nakagawa M, Tamanoi Y, Sato K. Direction control of primary jets using secondary flow near boundaries. Proceedings of the 28th Annual Meeting of the Kanto Branch of the Japan Society of Mechanical Engineers; 2022 Mar 14-15; Japan. (Online)
[5] Tezuka H, Nakagawa M, Zhang Q, Sato K. Directional control of jets near a boundary using coander secondary flow. The 21st International Symposium on Advanced Technology; 2022 Nov 24,25; Vietnam. (Online)
[6] Tezuka H, Zhang Q, Nishibe K, Sato K. Flow-direction control of primary jets near a wall boundary using secondary flow with a Coanda surface. 12th TSME-International Conference on Mechanical Engineering; 2022 Dec 13-16; Bangkok: Thailand. p. 400-406. (Online)
[7] Tezuka H, Zhang Q, Nishibe K, Sato K. Flow-Direction control of primary jets near a wall boundary using secondary flow with a coanda surface. J Res Appl Mech Eng. 2023;11(2):1-7.
[8] Borque C, Newman BG. Reattachment of a two-dimensional, incompressible jet to an adjacent flat plane. Aeronautical Quarterly. 1960;11(3):201-232.
[9] Hunter CA, Deere KA. Computational investigation of fluidic counterflow thrust vectoring. 35th AIAA/ASME/SAE/ASEE Joint Propulsion Conference & Exhibit; 1999 Jun 20-23; Los Angeles, United States. Reston: AIAA; 1999. p. 1-13.
[10] Shakouchi T. Jet flow engineering fundamentals and applications. Japan: Morikita Publishing; 2009.
[11] Trancossi M, Stewart J, Maharshi S, Angeli D. Mathematical model of a constructal Coanda effect nozzle. J Appl Fluid Mech. 2016;9(6):2813-2822.
[12] Al-Asady AAA, Abdullah AM. Fluidics thrust vectoring using co-flow method. Al-Nahrain J Eng Sci. 2017;20(1):5-18.
[13] Kobayashi R, Watanabe Y, Tamanoi Y, Nishibe K, Kang D, Sato K. Jet vectoring using secondary Coanda synthetic jets. Mech Eng J. 2020;7(5):1-16.
[14] Tamanoi Y, Kobayashi R, Sato K, Nishibe K, Kang D. Flow control using excited jets with coanda surfaces. The 31st International Symposium on Transport Phenomena; 2020 Oct 13-16; USA. (Online)
[15] Tamanoi Y, Watanabe Y, Kobayashi R, Sato K. Jet direction control using secondary flows. International Symposium on Transport Phenomena and Dynamics of Rotating Machinery; 2020 Nov 23-26; USA. (Online)
[16] Tamanoi Y, Sato K. Structure of jet deflected by secondary flow. The 20th International Symposium on Advanced Technology; 2021 Nov 23-24; Japan. (Online)
[17] Zhang Q, Takahashi F, Sato K, Tsuru W, Yokota K. Jet direction control using circular cylinder with tangential blowing. Trans Jpn Soc Aeronaut Space Sci. 2021;64(3):181-188.